Comparative investigation of InGaP/GaAs pseudomorphic field-effect transistors with triple doped-channel profiles

© Jung-Hui Tsai*¶, Der-Feng Guo+, Wen-Shiung Lour×

* Department of Electronic Engineering, National Kaohsiung Normal University, Kaohsiung 802, Taiwan
+ Department of Electronic Engineering, Air Force Academy, Kaohsiung, Taiwan
× Department of Electrical Engineering, National Taiwan Ocean University, Keelung, Taiwan

(Получена 15 февраля 2011 г. Принята к печати 22 февраля 2011 г.)

In this article, the comparison of DC performance on InGaP/GaAs pseudomorphic field-effect transistors with tripe doped-channel profiles is demonstrated. As compared to the uniform and high-medium-low doped-channel devices, the low-medium-high doped-channel device exhibits the broadest gate voltage swing and the best device linearity because more twodimensional electron gases are formed in the heaviest doped channel to enhance the magnitude of negative threshold voltage. Experimentally, the transconductance within 50% of its maximum value for gate voltage swing is 4.62 V in the low-medium-high doped-channel device, which is greater than 3.58 (3.30) V in the uniform (high-medium-low) doped-channel device.

1. Introduction

$A^{III}B^{IV}$ heterostructure field-effect transistors (HFETs) have been widely applied in signal amplifier and digital integrated circuits [1–3]. Among of the HFETs, the transconductance of high electron mobility transistors (HEMTs) may be relatively high resulting from the twodimensional electron gas (2DEG) in the modulated channel, however, they suffered from poor device linearity and low output current [4]. Transistor performances with high output current and linearity are especially essential for linear amplification in circuit applications. Over the past years, an alterable HFET, i. e., doping-channel FET (DCFET), has been investigated to exhibit broad gate voltage swing for improving the device linearity and reducing the higher order harmonic terms in linear amplifier applications [5–9]. A large bandgap InGaP undoped (or low-doped) material was employed as Schottky barrier layer in InGaP/GaAs DCFET, which could provide some advantages such as low DX centers, low reactivity of thermal oxidation, and high etching selectivity with GaAs material layer [7]. On the other hand, as considering the carrier conduction, replacing GaAs layer with InGaAs strain layer as a channel is appropriate because of the low effective electron mass, high electron mobility, and high peak electron velocity [5]. Nevertheless, it will give rise to compressive strain, and In more fraction as well as the thickness of InGaAs layer is critically limited due to the lattice mismacth with GaAs material [10].

In order to extend the thickness of InGaAs channel layer for enhancing drain current and device linearity, an $(Al_{0.3}Ga_{0.7})_{0.5}In_{0.5}P$/InGaAs pseudomorphic double-channel DCFET has been well demonstrated [9]. However, not any study related to the influence fo doping profiles on multiple-channel DCFETs is reported until now. In this article, three kinds of InGaP/InGaAs triple-channle field-effect transistors with different doped-channel profiles are investigated and compared. Among of the devices, the magnitude of negative threshold voltage is substantially extended and the gate voltage swing is effectively improved by the design of low-medium-high doped-channel profile.

2. Experiments

The studied device with low-medium-high doped-channel profile, labeled device A, was grown on an (100) oriented semiinsulating GaAs substrate by low-pressure metal-organic chemical-vapor deposition system (LR-MOCVD). The epitaxial structures consisted of a 0.3 μm undoped GaAs buffer layer, a 300 Å undoped $In_{0.49}Ga_{0.51}P$ layer, a 100 Å ($n^+ = 3.5 \cdot 10^{18}\,cm^{-3}$) $In_{0.15}Ga_{0.85}As$ lower doped-channel layer, a 50 Å undoped $In_{0.49}Ga_{0.51}P$ layer, a 100 Å ($n^+ = 2.5 \cdot 10^{18}\,cm^{-3}$) $In_{0.15}Ga_{0.85}As$ intermediate doped-channel layer, a 50 Å undoped $In_{0.49}Ga_{0.51}P$ layer, a 100 Å($n^+ = 1.5 \cdot 10^{18}\,cm^{-3}$) $In_{0.15}Ga_{0.85}As$ upper doped-channel layer, and a 200 Å undoped $In_{0.49}Ga_{0.51}P$ gate layer. Finally, a 300 Å ($n^+ = 1 \cdot 10^{19}\,cm^{-3}$) GaAs cap layer was deposited on the gate layer. Trimethylindium (TMI), trimethylgallium (TEG), phosphine (PH_3), and arsine (AsH_3) were used as the In, Ga, P, and As sourses, respectively. The dopants used for *n* and *p* layers were silane (SiH_4) and dimethylzine (DMZ), respectively. Drain and source ohmic contacts performed by evaporating AuGeNi metal and alloyed at 400°C for 30 s. Gate electrode was fabricated by evaporating Au metal on the 200 Å InGaP gate layer to from the gate Schottky contact. In addition, two similar devices were fabricated to compare the characteristics of the device A. The uniform doping device, labeled device B, has the identical doping level of $2.5 \cdot 10^{18}\,cm^{-3}$ in the triple channels. While in the high-medium-low doped-channel device, labeled device C,

¶ E-mail: jhtsai@nknucc.nknu.edu.tw

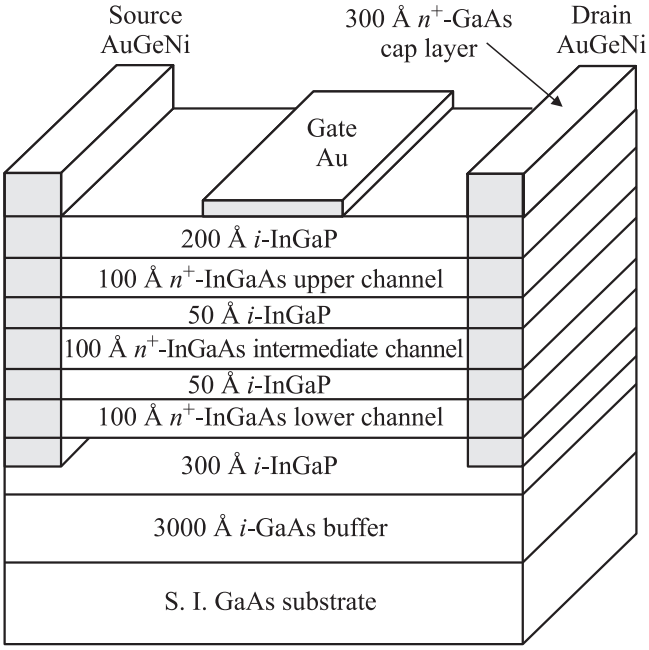

Fig. 1. Schematic cross sections of the InGaP/InGaAs triple-channel pseudomorphic field-effect transistors with different doped-channel profiles. Gate dimension and drain-to-sourcespacing were $1 \times 10\,\mu m^2$ and $3\,\mu$m, respectively.

the doping concentrations are of $3.0 \cdot 10^{18}$, $2.5 \cdot 10^{18}$, and $2.0 \cdot 10^{18}\,cm^{-3}$ in the upper, intermediate, and lower doped-channel layers, respectively. The schematic cross sections of the devices are shown in Fig. 1.

3. Experimental result and discussion

The corresponding conduction band daigrams at equilibrium by a twodimensional semiconductor simulation package, Atlas, are shown in Fig. 2. At this condition, the gate layer together with the upper doped layer is completed depleted while the gate depletion region extends part of the intermediate doped-channel layer in the three devices. Due to the presence of the considerable conduction band discontinuity at $In_{0.49}Ga_{0.51}P/In_{0.15}Ga_{0.85}As$ heterojunction [11], it provides a large potential barrier preventing the electron injection from channel into gate electrode under forward gate bias.

The experimental drain-to-source (DS) current-voltage characteristics are illustrated in Fig. 3. The applied forward gate voltage can reaches $+2$ V and the maximum drain saturation currents are of 90 mA for all of the devices. The large forward gate bias can be attributed from the large gate Schottky potential barrier and the well confinement effect for electron in each InGaAs channel between two undoped InGaP layers. It is worthy to note that the device A shows the largest drain current at $V_{GS} = 0$ and the largest magnitude of negative threshold voltage when compared with the other devices. These phenomena can be explained as follows. At equilibrium, the gate depleted region of the three devices immerses into the intermediate doped-channel layer and the lower doping channel layer maintains flat band, as seen in Fig. 2. It will form 2DEG in the lower InGaAs strain channel, which could increase the effective channel concentration [5]. In particular, the heavier the doping level in the lower strain channel is, the larger energy difference between conduction band and Femi level is. Thus, at equilibrium there are more 2DEGs formed in the lower

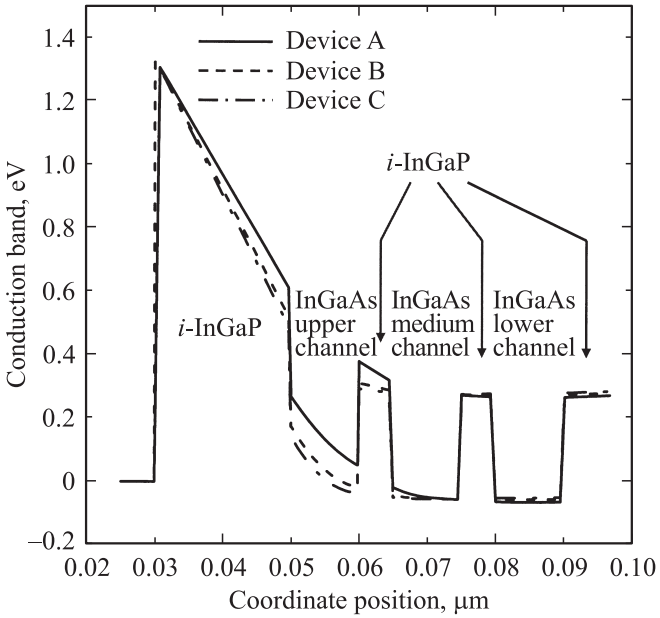

Fig. 2. Corresponding conduction band diagrams at equilibrium for the devices with different dope-channel profiles.

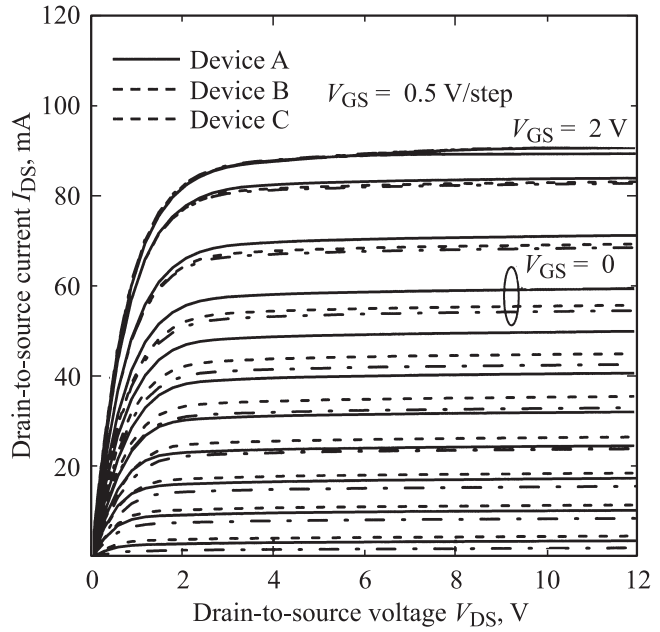

Fig. 3. Experimental drain-to-source current-voltage characteristics of the studied devices.

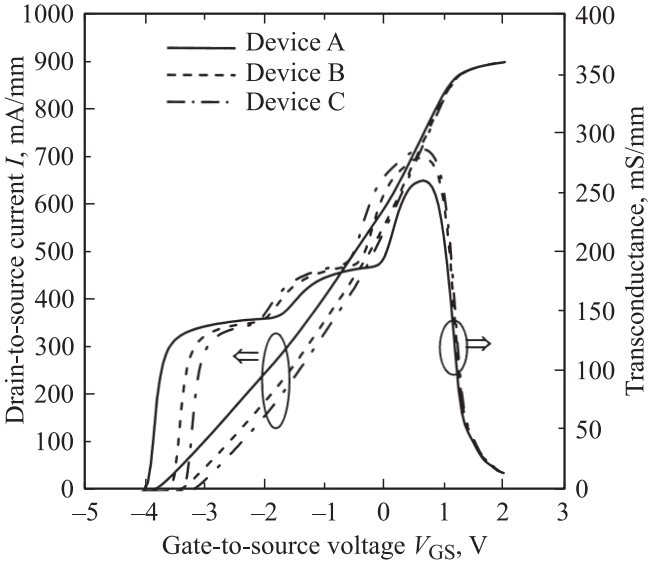

Fig. 4. Drain-to-source saturation current densities and transconductances versus gate voltage for the studied devices.

strain channel to enhance drain current for the device A, though the device has the largest gate depletion thickness. Furthermore, for the conventional depletion-mode DCFETs the drain saturation voltage $V_{D\,sat}$ at $V_{GS} = 0$ should be equal to the magnitude of threshold voltage. However, as V_{GS} is fixed at 0, the $V_{D\,sat}$ value is about 2.7 V in the three devices, which is smaller than the magnitudes of the negative threshold voltages. This means that the carrier modulation and 2DEGs in the InGaAs quantum well will be formed until the active channels are completely depleted.

The experimental DS saturation current densities and transconductances versus the applied gate voltage at $V_{DS} = +6$ V are illustrated in Fig. 4. The extrinsic transconductances of 262, 282, and 290 mS/mm are observed for the devices A, B, and C, respectively. Clearly, there are three linear regions appeared in the transfer characteristic due to the existence of the triple individual channel layers. The transconductance within 50% of its maximum value for gate voltage swing is 4.62 V (from $V_{GS} = -3.45$ to 1.17 V) in the device A, which is greater than 3.58 V (from $V_{GS} = -2.40$ to 1.18 V) in the device B and 3.30 V (from $V_{GS} = -2.10$ to 1.20 V) in the device C. Furthermore, as defining the drain current at 0.1 mA/mm, the threshold voltage is extended to -3.97 V in device A while they are only of -3.55 and -3.38 V in devices A and B, respectively. Therefore, the gate voltage swing and device linearity are substantially improved by the use of low-medium-high channel profile to extend magnitude of threshold voltage. In general, the transconductance value is inversely proportional to the gate depleted thickness. So, the maximum transconductance of device A is slightly lower than the other devices because the device A has the largest gate depleted thickness when the maximum transconductance appears.

4. Conclusion

The DC performance of InGaP/InGaAs triple-channel pseudomorphic field-effect transistors with different doped-channel profiles has been comparatively investigated. The low-medium-high doped-channel device exhibits the broadest gate voltage swing for broadening the magnitude of negative threshold voltage, though it has slightly lower transconductance than the other devices. Consequently, the demonstrated low-medium-high doped-channel device could provide a promise for linear amplification application.

This work was supported by the National Science Council of the Republic of China under Contract No, NSC 99-2221-E-017-018.

References

[1] Y.S. Lin, B.Y. Chen. J. Electrochem. Soc., **154**, H951 (2007).
[2] M.W. Pospieszalski. IEEE Microwave Magazine, **6**, 62 (2005).
[3] L.Y. Chen, H.I. Chen, C.C. Huang, Y.W. Huang, T.H. Tsai, Y.C. Liu, T.Y. Chen, S.Y. Cheng, W.C. liu. Appl. Phys. Lett., **95**, 052 105 (2009).
[4] S.J. Yu, W.C. Hsu, Y.J. Chen, C.L. Wu. Sol. St. Electron., **50**, 291 (2006).
[5] L.W. Laih, W.S. Lour, J.H. Tsai, W.C. Liu, C.Z. Wu, K.B. Thei, R.C. Liu. Sol. St. Electron., **39**, 15 (1995).
[6] J.H. Tsai, W.S. Lour, T.Y. Weng, C.M. Li. Semiconductors, **44**, 223 (2010).
[7] S.S. Lu, C.C. Meng, Y.S. Lin, H. Lan. IEEE Trans. Electron. Dev., **46**, 48 (1999).
[8] K.H. Su, W.C. Hsu, C.S. Lee, P.L. Hu, Y.H. Wu, L. Chang, R.S. Hsiao, J.F. Chen, T.W. Chi. Semicond. Sci. Technol., **23**, 045 012 (2008).
[9] S.C. Yang, H.C. Chin, F.T. Chien, Y.J. Chan, J.M. Kuo. IEEE Electron. Dev. Lett., **22**, 170 (2001).
[10] D.A. Ahmari, M.T. Fresina, Q.J. Hartmann, D.W. Barlage, P.J. Mares, M. Feng, G.E. Stillman. IEEE Electron. Dev. Lett., **17**, 226 (1996).
[11] J.H. Rsai, K.P. Zhu. Mater. Chem. Phys., **82**, 501 (2003).

Редактор Т.А. Полянская